

## ORIGINAL ARTICLE

# The Characterization and Regulation of Schwann Cells in the Tooth Germ Development and Odontogenic Differentiation

Jing He<sup>1,2,\*</sup>, Ting Wang<sup>1,3,\*</sup>, Danyang Liu<sup>1,4</sup>, Jun Yang<sup>1</sup>, Yuanpei He<sup>1</sup>, Shouliang Zhao<sup>1</sup>, Yanqin Ju<sup>1</sup>

<sup>1</sup>Department of Stomatology, Huashan Hospital, Fudan University, Shanghai, China

<sup>2</sup>Faculty of Dentistry, The University of Hong Kong, Hong Kong, China

<sup>3</sup>Shanghai Jingan Dental Clinic, Shanghai, China

<sup>4</sup>Department of Stomatology, Tongren Hospital, Shanghai Jiao Tong University School of Medicine, Shanghai, China

Schwann cells (SCs), a type of glial cell in the peripheral nervous system, can serve as a source of mesenchymal stem cells (MSCs) to repair injured pulp. This study aimed to investigate the role of SCs in tooth germ development and repair of pulp injury. We performed RNA-seq and immunofluorescent staining on tooth germs at different developmental stages. The effect of L-type calcium channel (LTCC) blocker nimodipine on SCs odontogenic differentiation was analyzed by real-time polymerase chain reaction and Alizarin Red S staining. We used the PLP1-CreERT2/Rosa26-GFP tracing mice model to examine the role of SCs and Ca<sub>v</sub>1.2 in self-repair after pulp injury. SC-specific markers expressed in rat tooth germs at different developmental stages. Nimodipine treatment enhanced mRNA levels of osteogenic markers (DSPP, DMP1, and Runx2) but decreased calcium nodule formation. SCs-derived cells increased following pulp injury and Ca<sub>v</sub>1.2 showed a similar response pattern as SCs. The different SCs phenotypes are coordinated in the whole process to ensure tooth development. Blocking the LTCC with nimodipine promoted SCs odontogenic differentiation. Moreover, SCs participate in the process of injured dental pulp repair as a source of MSCs, and Ca<sub>v</sub>1.2 may regulate this process.

**Keywords:** Schwann cells, Tooth development, Ca<sub>v</sub>1.2, Odontogenic differentiation, Pulp injuries

## Introduction

Dental development is a complex and reciprocal process

Received: December 27, 2023, Revised: April 23, 2024,  
Accepted: May 31, 2024, Published online: July 29, 2024

Correspondence to **Yanqin Ju**

Department of Stomatology, Huashan Hospital, Fudan University,  
12 Urumqi Road, Shanghai 200040, China  
E-mail: yanqin\_ju@fudan.edu.cn

Co-Correspondence to **Shouliang Zhao**

Department of Stomatology, Huashan Hospital, Fudan University,  
12 Urumqi Road, Shanghai 200040, China  
E-mail: slzhao@fudan.edu.cn

\*These authors contributed equally to this work.

© This is an open-access article distributed under the terms of the Creative Commons Attribution Non-Commercial License (<http://creativecommons.org/licenses/by-nc/4.0/>), which permits unrestricted non-commercial use, distribution, and reproduction in any medium, provided the original work is properly cited.

Copyright © 2024 by the Korean Society for Stem Cell Research

between epithelial and mesenchymal, including tooth morphogenesis, hard tissue differentiation and mineralization, root formation and eruption. The neural crest ectomesenchyme gives rise to the cells that eventually form the tooth (1). Furthermore, neural crest-derived cells, Schwann cell precursors (SCPs) and Schwann cells (SCs) have been shown to maintain mesenchymal stem cell reservoir and participate in the tooth growth and development (2). SCs, as the major glial cell type of the peripheral nerve system (PNS), originate from the neural crest in a well-defined development step. Neural crest cells developed into SCs and then converted into immature SCs (iSCs). iSCs differentiated into myelinated SCs (mSCs) and non-myelinated SCs (nmSCs) through the radial sorting (3). The phenotypic plasticity of SCs plays essential roles in the normal development of peripheral nerves and the response to nerve injury. It is commonly recognized that dental pulp tissue is densely packed with nerve fibers and requires a conti-

nuous supply of nerve cells. SCs, as one of the progenitor cells of dental-derived stem cells and major glial cell type of PNS (2), are believed to contribute to tooth development and injury repair. However, there are limited studies regarding the phenotypes and phenotype change of SCs during tooth development. The factors that affect the participation of SCs in pulp injury repair are also not fully understood.

Calcium, as an intracellular messenger, regulates cell growth, differentiation and apoptosis. L-type calcium channel (LTCC) is a transmembrane protein involved in several biological processes varying from neurogenesis (4), osteogenesis (5), and cardiomyogenesis (6). Our previous studies found that  $Ca_v1.2$  was the primary type of LTCC expressed in the human dental pulp and plays a significant role in the odontogenic differentiation of dental pulp cells (7) and  $NG2^+$  pericytes (8).  $Ca_v1.2$  is also found abundantly expressed in nerve fibers, SCs and astrocytes during the repair and regeneration of the pulp after tooth injury (9). Thus, we hypothesize that  $Ca_v1.2$  also plays an essential role in SCs odontogenic differentiation and participates in the renewal of dentine after damage. Our previous study has successfully established the induction of SCs into odontoblasts *in vitro* (10). In the present study, we used the same odontogenic induction method (10) to induce SCs into odontoblasts while using the LTCC blocker nimodipine to interfere with the expression of  $Ca_v1.2$ . In addition, we performed the incisor injury in the PLP1-CreERT2/Rosa26-GFP tracing mice model, which can trace the SCs and their daughter cells. And then  $Ca_v1.2$  immunofluorescence staining was applied to the injured incisors.

Therefore, the present study sought to clarify the phenotypes of SCs at different stages of tooth germ development. Furthermore, we investigated whether  $Ca_v1.2$  functions in SCs odontogenic differentiation process *in vitro* and how SCs participate in self-repair following pulp injury.

## Materials and Methods

### RNA-seq and protein-protein interaction network analysis

We extract the cellular RNA from the tooth germ cells of rats at different phases (E14.5, E16.5, E18.5, P1, and P7) using Trizol reagent (Invitrogen) to construct a cDNA library. The construction of each cDNA library was implemented following the manufacturer's suggestions, and next-generation sequencing was carried out using an Illumina HiSeq 2000 platform (IGA). RNA-seq analysis was conducted to identify and visualize the expression of differentially expressed genes (DEGs) involved in tooth germ development. Besides, we established the protein-protein

interactions (PPIs) network by integrating protein information from the Search Tool for the Retrieval of Interacting Genes database (<https://string-db.org/>) to further explore the relationships among the DEGs at the protein level.

### Acquisition of rats' mandibular first molar specimens in the different development periods

We chose 12-week-old Sprague-Dawley rats for the study. Rats were housed under a 12 : 12 light-dark cycle with free access to food and water. All procedures used in this study were conducted in accordance with the Animal Care Committee for the Care and Use of Laboratory Animals of Fudan University. The female mice were mated with male mice at a ratio of 2 : 1. Then we checked the progesterone plugs and regarded the noon that progesterone plugs appeared as embryonic development at 0.5 day. We select pregnant mice that 14.5 days, 16.5 days, and 18.5 days pregnancy (i.e., E14.5, E16.5, E18.5) and mice that 1 day, 7 days and 10 days postnatal (i.e., P1, P7, P10) as research objects. Pregnant SD rats in different periods were given intraperitoneal anesthesia (10% chloral hydrate, 0.5 mL/100 g). Then we checked the anesthesia effect 15 minutes later. After that, we opened the abdomen along the abdominal midline and exposed the uterus. We were lifting up the cervix of the uterus with forceps and exposing beaded fetal rats. Then we placed them gently on plates full of phosphate buffer saline (PBS). Afterwards, we washed them off and evacuated the placenta and tear membrane. Then we separated fetal rat heads, washed them off with PBS again and fixed them in 4% paraformaldehyde solution (PFA). SD rats at P1 were sacrificed, separated heads, washed off with PBS and fixed in 4% PFA. SD rats at P7 were sacrificed, separated heads and washed off with PBS. Then we removed the mandible integrally along the bilateral auriculotemporal region, washed them off and fixed them in 4% PFA for more than 48 hours. After that, we washed the mandible off with PBS many times, immersed them in 10% ethylene diamine tetraacetic acid (EDTA) which was 20 times the volume of the mandible and replaced the solution every two days. The mandible was decalcified until it was like rubber, elastic and easily through by pin. Then we washed off the separated heads of different periods in PFA and mandible in EDTA with flowing water for 4 hours, placed them in 75% ethanol overnight, dehydrated them the next day and embedded them in paraffin. Then these paraffin specimens were sectioned in the coronal plane and the slice thickness was 5  $\mu$ m. All experiments were approved by the Ethical Review Committee of Fudan University (Shanghai, China) (approval no. JS-178).

### Odontogenic differentiation

SCs were seeded at a density of 5,000 cells/cm<sup>2</sup> in 6-well plates and cultured overnight in Schwann cell medium (SCM; ScienCell) (Supplementary Methods). At about 60% confluence, SCM was replaced with odontogenic differentiation medium (ODM), which consisted of  $\alpha$ -minimal essential medium (HyClone), 10% FBS (ScienCell), 5 mmol/L glycerol-2-phosphate (Sigma-Aldrich), 10 nmol/L dexamethasones (Sigma-Aldrich), 50  $\mu$ g/mL ascorbic acid (Sigma-Aldrich), 100 U/mL penicillin (Sigma-Aldrich), 100 U/mL streptomycins (Sigma-Aldrich), with or without nimodipine (Bayer). All solutions were freshly prepared immediately before use. The medium was changed every 3 days.

### Immunofluorescence staining

SCs were cultured on the 24-well plates with a cell culture slide. After removing the medium, cells were washed with PBS and fixed with 4% paraformaldehyde. Subsequently, the slides were treated with 0.3% Triton X-100. The cells were blocked with 5% BSA. Specific primary antibodies targeting each marker (S100 [1 : 200; Abcam]; dentin sialoprotein [DSP, 1 : 50; Santa Cruz Biotechnology]; Ca<sub>v</sub>1.2 [1 : 50; Santa Cruz Biotechnology]) were added at different concentrations. The slides were incubated overnight at 4°C and washed twice with PBS, then incubated with the secondary antibody (Alexa Fluor 594 AffiniPure goat anti-rabbit IgG, 1 : 200; Jackson ImmunoResearch) for 2 hours at room temperature (RT). After the nuclei were visualized by 4',6-diamidino-2-phenylindole (DAPI, 1 : 1,000; Calbiochem), the slides were analyzed with a microscope (Eclipse 80i; Nikon).

### Real-time polymerase chain reaction

Total RNA was extracted using TRIzol (Invitrogen) from the cells cultured in the SCM and ODM with or without nimodipine for 14 days. Approximately 2  $\mu$ g total RNA was used to synthesize cDNA using the RevertAid First-strand cDNA Synthesis Kit (Thermo Scientific). Odontogenesis was evaluated in the SCs based on the expression of specific genes (*DSPP*, *DMP-1*, *Runx2*). Glyceraldehyde-3-phosphate dehydrogenase (GADPH) was used as the control to normalize the RNA expression levels. Real-time polymerase chain reaction (PCR) was performed by using an ABI 7500 real-time PCR system (Applied Biosystem) and the SYBR green SuperReal PreMix Plus (FP205; Tiangen). Subsequently, a Ct value was obtained for each sample. The fold change in gene expression relative to the control was calculated using the  $2^{-\Delta\Delta Ct}$  method. The primer sequences used in the real-time PCR are listed in Supplementary Table S1.

### Alizarin Red S staining and quantification

Alizarin Red S staining was used to examine calcium phosphate formation after 28 days of odontogenic differentiation. After removing ODM, the cells were gently washed with PBS and fixed with 4% paraformaldehyde for 15 minutes at RT, followed by washing with PBS and stained with a 0.2% Alizarin Red S (pH 4.2) (Sigma-Aldrich) for 30 minutes in the dark. Then excess dye was removed by repeated washing with PBS.

### Establishment of mice pulp injury model

Induced model mice were given intraperitoneal anesthesia with 2% pentobarbital sodium (80 mg/kg) and ground right mandibular incisor for 2 mm with a high-speed air turbine drill. The left mandibular incisor was taken as a control group. We chose the right incisors at different time points after injury (0, 2, 6, 12, 24, 48, 72 hours, 5 days, and 1 week) for observation. We kept the mice warm and avoided hypothermia during the whole period.

### Acquisition of specimen of pulp injury model

Mice of the pulp injury model were allowed to survive for 0, 2, 6, 12, 24, 48, 72 hours, 5 days, and 1 week. After each survival period, mice were anesthetized with 2% pentobarbital sodium (80 mg/kg) and fixed by cardiac perfusion with 4% PFA. After that, mandibles with incisors were extracted completely, and excess soft tissue was removed. Then mandibles were further fixed in 4% PFA overnight. 24 hours later, mandibles were washed off with PBS and immersed in 10% EDTA which was 20 times the volume of the mandible. The decalcifying solution was changed every two days. The completion of the decalcification-mandible was elastic and easily through by pin-specimens were washed off with PBS and embedded in paraffin, sectioned in the coronal plane at a thickness of 5  $\mu$ m.

### Immunohistochemical and immunofluorescence staining

Immunohistochemical and immunofluorescence staining used standard protocol on 5  $\mu$ m coronal paraffin sections of the embryonic heads and mice mandibles. Primary antibodies were applied to the tissue and incubated at 4°C overnight. Primary antibodies were MBP101 (1 : 150, ab62631; Abcam), S100 $\beta$  (1 : 200, ab52642; Abcam), growth-associated protein 43 (GAP43, 1 : 200, ab75810; Abcam), Ki67 (1 : 100, ab15580; Abcam), green fluorescent protein (GFP, 1 : 200; Cell Signaling Technology), anti-Ca<sub>v</sub>1.2 (1 : 200; Alomone Labs), CY3 (1 : 200; Abcam) and Dylight 488 (1 : 200; Abcam) secondary antibodies were used. And additional staining was done with DAPI

(KeyGEN BioTECH). Dako solution was used to prevent quenching.

**Statistical analysis**

GraphPad Prism 7.0 software was used for all statistical analyses presented. Statistical significance was determined by using a one-way ANOVA. Each number was displayed as the mean±SD, and p<0.05 was considered statistically significant.

**Results**

**RNA-seq and PPIs network analysis**

The examined embryonic and postnatal stages were

E14.5, E16.5, E18.5, P1, and P7, representing the bud stage, cap stage, early bell stage, late bell stage and hard tissues formation stage, respectively. H&E staining results showed a significant morphological change as time went on (Supplementary Fig. S1). RNA-seq was constructed in different stages (E14.5, E16.5, E18.5, P1, and P7) of tooth germ development. DEGs associated with nervous system development were shown in Supplementary Data 1. Based on the PPIs network analysis, we found that genes related to the nervous system play an important role in the whole process of tooth germ development (Fig. 1A). Previous studies showed that SCs exist in different phenotypes, which have various molecular markers (Supplementary Table S2). We analyzed genes associated with SCs specific mark-

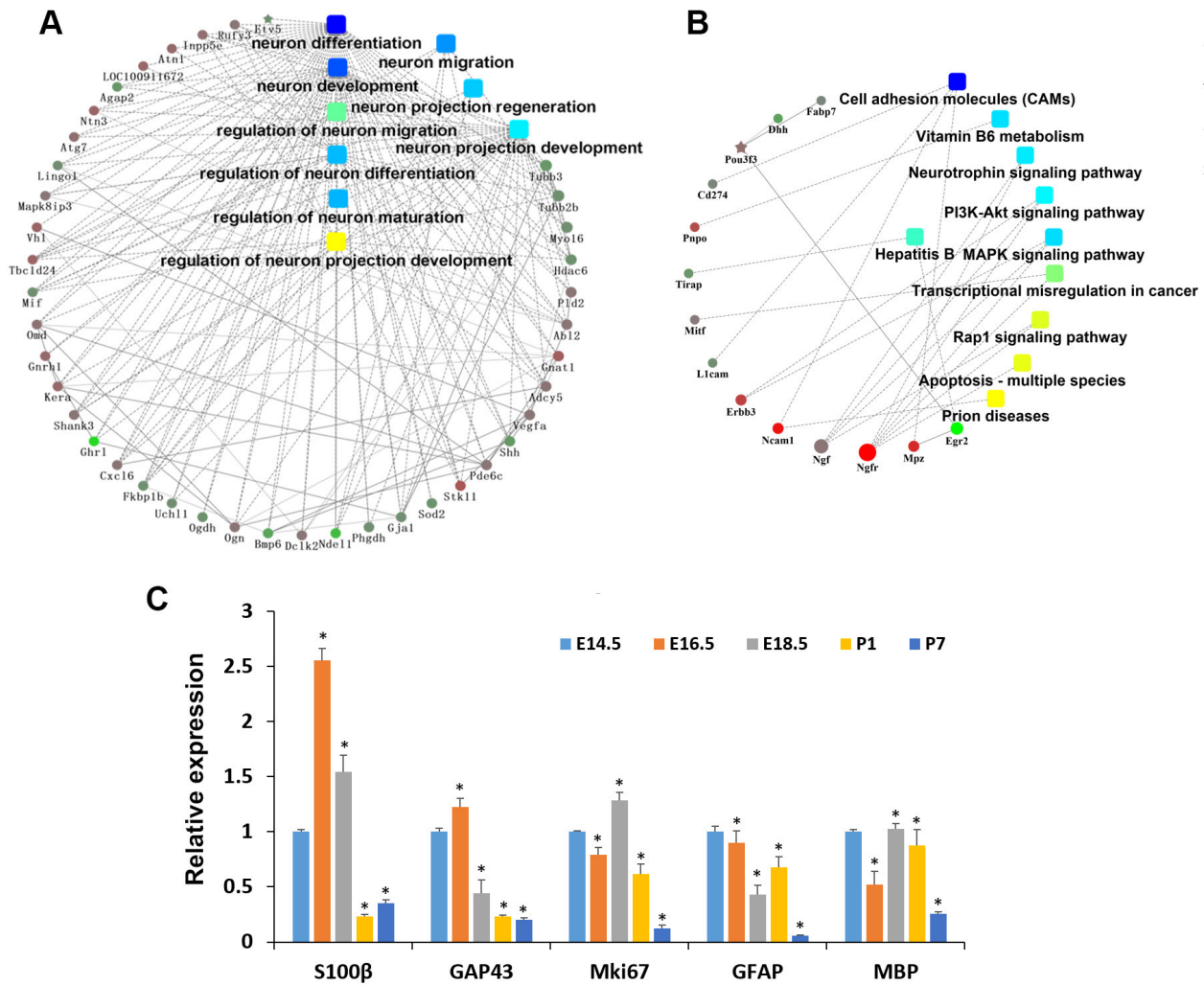


**Fig. 1.** Protein-protein interactions network and RNA-seq analysis. (A) Protein-protein interaction network of the differentially expressed genes of rat nervous system of tooth germ between E14.5 and P7 by RNA-seq. (B) Protein-protein interaction network of the differentially expressed genes associated with specific markers of the different phenotypes of Schwann cells between E14.5 and P7. (C) Differential expression of rat neural development marker of tooth germ by RNA-seq. \*p<0.05.

ers to validate the effect of SCs in tooth germ development. Results showed that they vary in the expression level in different developmental stages of tooth germs (Supplementary Table S3). Then we chose genes that existed in different phenotypes of SCs (specific markers) and carried out a PPI network analysis (Fig. 1B). The development of tooth germs may be significantly impacted by nerve growth factor, nerve growth factor receptor (also known as p75NTR), and cell adhesion molecules.

Among the genes primarily associated with cell proliferation, neuron growth and SCs development, we analyzed the expression of five marker genes, i.e., Mki67, GAP43, S100 $\beta$ , glial fibrillary acidic protein (GFAP) and myelin basic protein (MBP), which displayed dynamic expressions during various SCs development stages (Fig. 1C). Specifically, Mki67, a marker of proliferation Ki67, is linked to cell division (11); GAP43 is a neuronal growth-associated protein, highly expressed during the development and regeneration of nerves (12). S100 $\beta$  is a Ca<sup>2+</sup>-binding protein predominantly found in astrocytes in the central nervous system (CNS) and SCs (13). It is present in all SCs stages except for SCPs (14). GFAP is uniquely found in astrocytes in the CNS, non-myelinating SCs in the PNS, and enteric glial cells. It emerges at a relatively late stage in SCs development, mainly expressed in iSCs during embryonic development and nmSCs after birth (15). MBP is mainly found in the oligodendrocytes in CNS and mSCs in the PNS (16,

17). Consequently, it may be reasonable to suggest that the expressions of S100 $\beta$ , GFAP, and GAP43 in the tooth germs were contributed by SCs.

The dynamic expressions of GAP43 indicated that the neuron growth activity reached its peak at E16.5 during tooth development within the tooth germs. The expression of Mki67 was considerably higher between E14.5 and P1, suggesting that a majority of cells in tooth germs may be in a proliferative state before P7. S100 $\beta$ , GFAP and GAP43 exhibited distinct expressions and trends, but they partially overlapped at various stages of tooth germ development (Fig. 1C). Given different phenotypic SCs possess diverse yet overlapping molecular markers (Supplementary Table S2), we postulate that the plasticity of SCs is present and may play a crucial role in tooth development.

### Immunofluorescence staining of S100 $\beta$ , MBP101, GAP43, and Ki67

Three specific markers (S100 $\beta$ , MBP101, and GAP43) were chosen to characterize SCs in tooth development. SCPs (S100 $\beta$ <sup>-</sup>/GAP43<sup>+</sup>/MBP101<sup>-</sup>), iSCs/nmSCs (S100 $\beta$ <sup>+</sup>/GAP43<sup>+</sup>/MBP101<sup>-</sup>) and mSCs (S100 $\beta$ <sup>+</sup>/GAP43<sup>-</sup>/MBP101<sup>+</sup>) were recognized from E14.5 to P7 during the rat tooth germ development.

On E14.5, the tooth germ of the rat mandibular first molar was in the bud stage (Supplementary Fig. S1A). Epithelial cells proliferated into ectomesenchyme in which cells al-

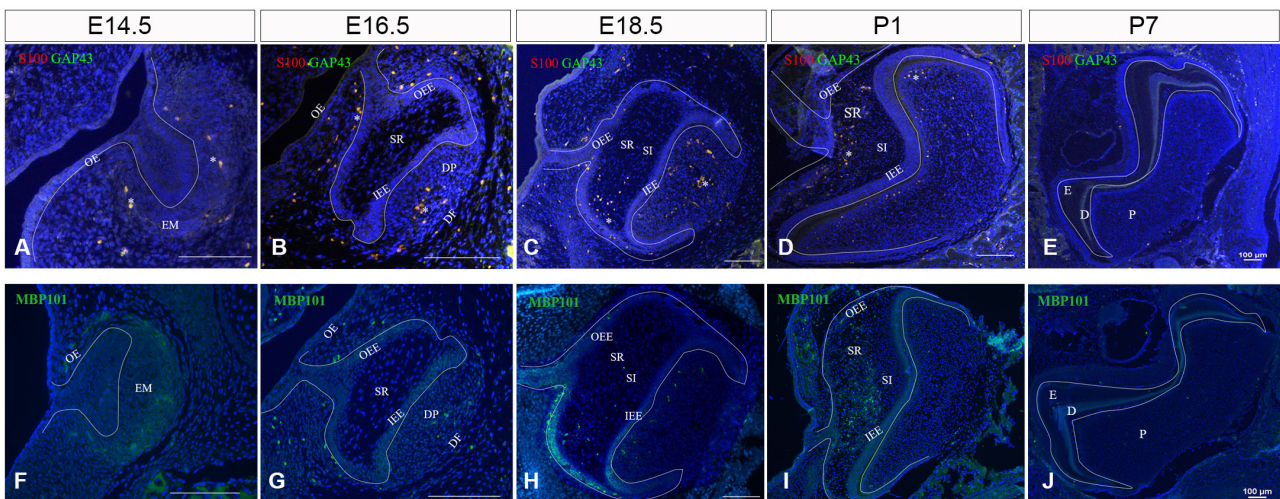


**Fig. 2.** Expression of rat neural development markers (GAP43, MBP101, S100 $\beta$ ) in tooth germ at different stages. (A, F) Neural development markers expression on E14.5, amplification times is 400 $\times$ . (B, G) Expression of neural development markers on E16.5, amplification times is 400 $\times$ . (C, H) Expression of neural development markers on E18.5, amplification times is 200 $\times$ . (D, I) Expression of neural development markers at P1. (E, J) Expression of rat neural development markers in tooth germ on P7. DAPI in blue. S100: S100 $\beta$ , OE: outer enamel, EM: ectodermal mesenchyme, OEE: outer enamel epithelium, SR: stellate reticulum, IEE: inner enamel epithelium, DP: dental papilla, DF: dental follicle, SI: stratum intermedium, E: enamel, D: dentin, P: dental pulp. \*Co-stained.

so proliferated but did not differentiate, forming the tooth bud. S100 $\beta$  and GAP43 were expressed in ectomesenchyme, while MBP101 had weak expression in the mesenchyme (Fig. 2A, 2F). And the weak expression of Ki67 could be seen in every part of this stage (Supplementary Fig. S2A).

On E16.5, the tooth germ of the rat mandibular molar was in the cap stage (Supplementary Fig. S1B). Epithelial cells continued to proliferate, and the tooth bud changed to the shape of the cap and became an enamel organ. This period enamel organ consists of 3 layers of cells: outer enamel epithelium (OEE), inner enamel epithelium (IEE), and stellate reticulum (SR). Below the enamel organ, there was a cell coacervation area called dental papilla (DP), which would develop into dentin and pulp. The ectodermal mesenchymal cells surrounding the enamel organ and the edge of DP are densely packed into the connective tissue layer to form the dental follicle (also known as dental sac) (DF). And enamel knots began to form. S100 and GAP43 co-expressed in the OEE, IEE, mesenchyme, and DF throughout this time period. Strong expression was detected in the DP, while weak expression was seen in the dental lamina (DL) and SR. Furthermore, MBP101 was expressed weakly in mesenchyme at this time period (Fig. 2B, 2G). Ki67 expression was stronger than E14.5 (Supplementary Fig. S2B, S2C).

On E18.5, the enamel organ turned into the bell stage (Supplementary Fig. S1C). Ameloblasts and odontoblasts began to differentiate. There were 4 layers in the enamel organ, i.e., OEE, IEE, SR, and stratum intermedium (SI). The enamel organ continued to extend and enfolded DP. At this stage, the expressions of S100 $\beta$  and GAP43 were strong in DP and DF, but weak in IEE, OEE, and DL. And there was almost no expression of them in SR and SI. MBP101 expressed strongly in DP and DF, sporadically in SR, and almost none in the other part of the enamel organ (Fig. 2C, 2H). The signal of Ki67 was much greater than before (Supplementary Fig. S2D).

On P1, the tooth germ progressed to the late bell stage (Supplementary Fig. S1D). The enamel organ still consists of 4 layers of cells. IEE differentiated into ameloblasts, and DP cells near IEE became odontoblasts. Ameloblasts and odontoblasts secreted enamel and dentin matrices. And there was a little predentin formed. S100 $\beta$  and GAP43 had scattered expressions in DP but expressed strongly in SR. There was no expression in the other locations (Fig. 2D, Supplementary Fig. S3). MBP101 had a similar expression pattern to them (Fig. 2I). Besides, the expression of Ki67 achieved a peak at this stage (Supplementary Fig. S2E-S2H).

On P7, tooth germ was forming the hard tissue. Tooth roots began to form since P1. SR gradually disappeared,

while SI still existed. Ameloblasts aggregated in IEE. Apparent enamel, dentin, and pulp formed (Supplementary Fig. S1E), and dentin thickened, and Hertwig epithelial root sheath formed on P10 (Supplementary Fig. S1F). During this period, the first molar was involved in the process of hard tissue formation (Fig. 2E, 2J). S100 $\beta$  and GAP43 are mostly expressed in the odontoblasts layer and co-expressed in the central and apical areas of the dental pulp (Fig. 2E, Supplementary Fig. S4). MBP101, on the other hand, is scattered in the dental pulp (Fig. 2J). Ki67 expression decreased in comparison to that in the early tooth germ development stage (Supplementary Fig. S5). The selected area in Supplementary Fig. S5A for observation was the odontoblasts of the pulp horn (Supplementary Fig. S5B), the central area of the pulp (Supplementary Fig. S5C), and the apical area (Supplementary Fig. S5D).

Briefly summary, the results showed that iSCs/nmSCs exist in ectomesenchyme, IEE, OEE, mesenchyme, DF, and most DP, whereas mSCs exist in mesenchyme. Developing into the bell stage, there are a large number of iSCs/nmSCs in DP and DF, but only small quantities in IEE, OEE and DL. And there was almost no existence in SR and SI. At the same time, mSCs exist most in DP and DF. Entering the late bell stage, a small number of iSCs/nmSCs and mSCs exist in DP, particularly in the odontoblast layer but a considerable number exist in SR. When the tooth germ is in the stage of hard tissue formation, iSCs/nmSCs are mostly found in the odontoblast layer and merely in the center of the dental pulp and the cusp. mSCs are scattered in the dental pulp. There was no obvious expression of SCPs found in the five time points studied in the present study.

### Blocking the LTCCs promoted the odontogenic differentiation of SCs

The cultured cells appeared with a fusiform morphology and showed two neurites and a small cell body, positively expressing S100, a phenotypic marker of SCs. We also observed the positive Ca<sub>v</sub>1.2 expression in SCs (Supplementary Fig. S6A). To examine the role of LTCC in the odontogenic differentiation of SCs, we used nimodipine to block LTCC. Different concentrations of nimodipine were added to SCM to determine its effect on the growing proliferation of SCs (Supplementary Methods). The cell proliferation curve showed that nimodipine had no significant effect on the proliferation of SCs compared with control during the first 5 days. After 7 days, high doses of nimodipine (2.5, 5, and 10  $\mu$ M nimodipine) might gradually inhibit cellular proliferation. In contrast, 0.1 and 1  $\mu$ M nimodipine had no significant effect on SCs

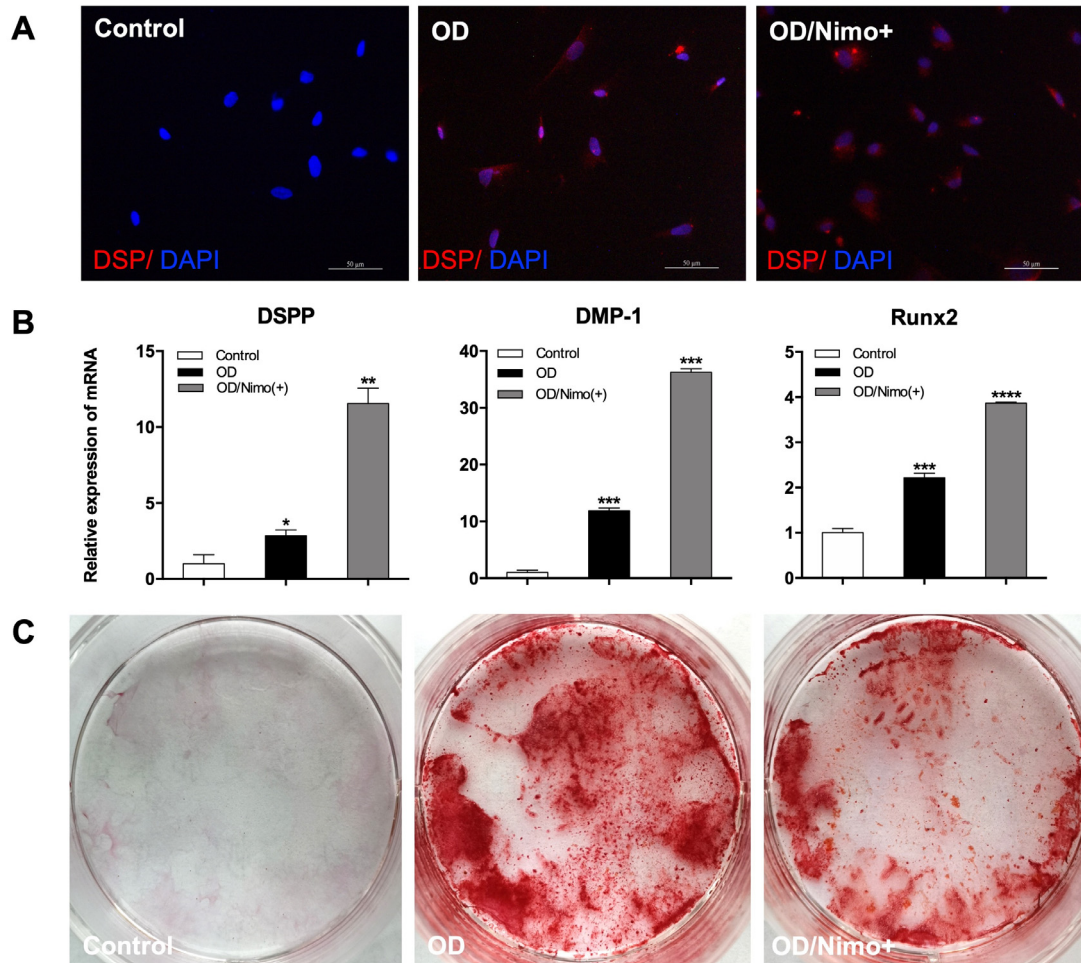


**Fig. 3.** Effects of L-type calcium channel on the odontogenic differentiation of Schwann cells (SCs) *in vitro*. (A) Immunofluorescence staining of DSP in SCs after odontogenic differentiation. Scale bar=50  $\mu$ m. (B) The mRNA expression of DSPP, DMP-1 and Runx2 in the three groups was measured at 14 days by real-time polymerase chain reaction. (i) Control: SCs in Schwann cell medium. (ii) OD: SCs in odontogenic differentiation medium (ODM). (iii) OD/Nimo(+): SCs in ODM supplemented with 1  $\mu$ M nimodipine. Error bar:  $\pm$ SD (n=3); \*p<0.05, \*\*p<0.01, \*\*\*p<0.001, \*\*\*\*p<0.0001 OD group with or without nimodipine versus control. (C) Images of Alizarin Red S staining at 28 days of odontogenic differentiation.

growth (Supplementary Fig. S6B). Therefore, 1  $\mu$ M nimodipine was used to inhibit LTCC during the odontogenic differentiation of SCs.

DSP, a specific marker of odontoblasts, was positive in both OD groups with or without nimodipine treatment after odontogenic differentiation for 14 days but negative in the control group (Fig. 3A). Real-time PCR results showed that the expression of *DSPP*, *DMP-1*, and *Runx2* had significantly increased in the OD group compared with the control group (p<0.05, n=3). After treatment with nimodipine for 14 days, the expression of all these odontogenesis-specific genes in the OD group with nimodipine was higher than that in the OD group (p<0.05, n=3) (Fig. 3B). Additionally, calcium nodules were observed in the OD

group via Alizarin Red S staining at 28 days after odontogenic differentiation. Interestingly, calcium nodule formation was reduced by the addition of nimodipine (Fig. 3C).

### SCs-derived cells and Ca<sub>v</sub>1.2 participated in the regeneration of incisors after injury

To examine whether SCs-derived cells could produce regenerative dentine after injury, we used PLP1-CreERT2/Rosa26-GFP mice to trace SCs and progeny (Supplementary Methods). According to the Jackson Laboratory instructions, we performed the mice genotype detection and got PLP1-CreERT2/Rosa26-GFP mice (Supplementary Fig. S7A), in which SCs and progeny were labelled by GFP after Tamoxifen induction. During the repair time, we ob-

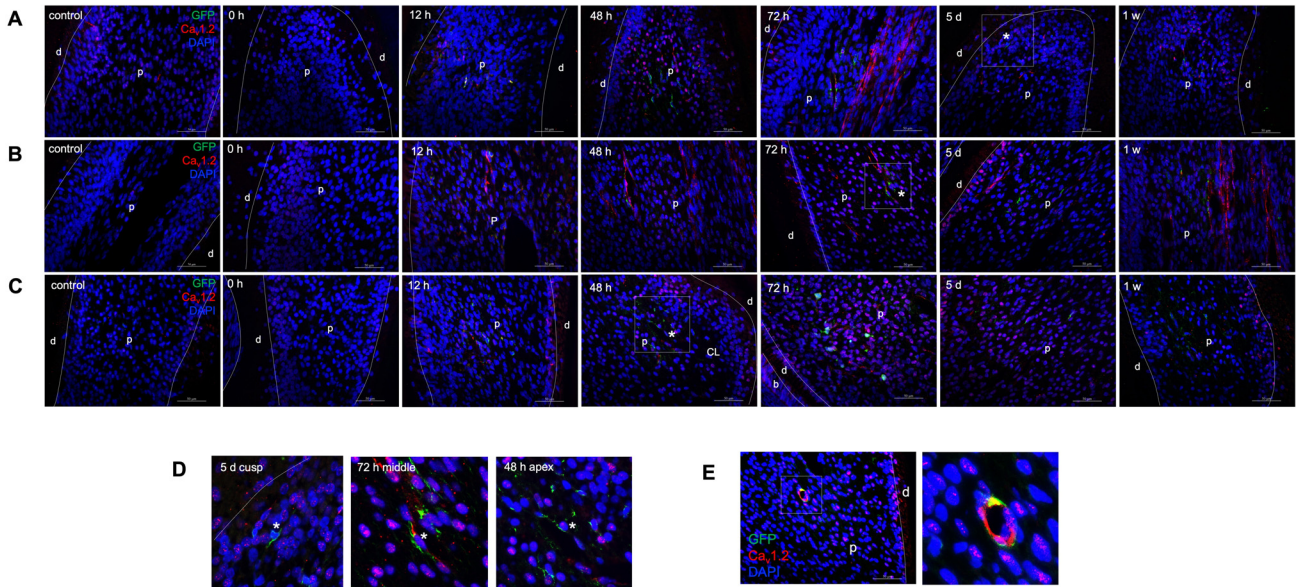


**Fig. 4.** SCs-derived cells and  $Ca_v1.2$  participate in the regeneration of incisors after injury. (A-C) represent the expression of  $GFP^+$  cells (green) and  $Ca_v1.2$  (red) at the dental cusp, middle teeth and apical area of control and injured incisors with recovery for 0, 12, 48, 72 hours, 5 days, and 1 week, respectively. Boxed areas are shown magnified in (D) correspondingly. (D) The possible route of SCs-derived cells migrating to the odontoblast layer. The asterisk highlights  $GFP^+$  cells. (E) Co-expression of  $GFP^+$  cells and  $Ca_v1.2$ . Boxed areas are shown magnified to the right. Scale bar = 50  $\mu$ m. d: dentin, p: dental pulp, CL: cervical loop.

served that the mice's left mandibular incisors length recovered to control length within one week after injury (Supplementary Fig. S7B). Therefore, we observed the changes in the expression of SCs and  $Ca_v1.2$  in the pulp of mice after incisor injury within one week. The immunostaining results indicated almost no  $GFP^+$  cells (SCs and their progeny) in the cusp, middle and apex of control incisors, similar to that injured group (0 hour) without recovery. However, as the recovery time progressed,  $GFP^+$  cells increased gradually, and they were most visible at 48 and 72 hours after injury (Fig. 4A-4C) but weak at other time points (Fig. 4A-4C, Supplementary Fig. S7C-S7E). Notably, after 48 hours of recovery, some  $GFP^+$  cells migrated from the apex to the cusp of incisors and existed at the odontoblasts layer near the injured site at 5 days after injury (Fig. 4D), indicating that SCs could differentiate into odontoblasts to produce regenerative dentin after injury.

$Ca_v1.2$  channel expression was also investigated at the same time points following injury. In the tooth cusps, we observed a marked decrease in the  $Ca_v1.2$  staining from 0 to 24 hours after injury compared to the non-injured control group. Starting from 48 hours after injury, its staining was enhanced gradually (Fig. 4A, Supplementary Fig. S7C). In the middle of tooth,  $Ca_v1.2$  was almost absent from the odontoblast layer and pulp cells, however, the lo-

calization of  $Ca_v1.2$  returned after injury and increased gradually, with the highest expression at 72 hours and then kept stable (Fig. 4B, Supplementary Fig. S7D). At the apex, there was a small amount of  $Ca_v1.2$  expression in the control, 0 and 2 hours groups, but there was no significant difference among these three groups. By 6 hours after injury,  $Ca_v1.2$  expression increased gradually, peaking at 72 hours and subsequently declined (Fig. 4C, Supplementary Fig. S7E).

The expression trends of SCs and  $Ca_v1.2$  were similar. Both showed a notable strong staining pattern at 48 and 72 hours after injury. We also detected the co-staining of SCs ( $GFP^+$ ) and  $Ca_v1.2$  (red). Regions of overlap were shown in yellow in the neurovascular bundle (Fig. 4E), indicating that  $Ca_v1.2$  may be involved in the process of SCs participating in dentin regeneration after injury.

## Discussion

Neural crest cells are multipotent cells that contribute to generating most of the cell types for the peripheral nervous system (PNS) during the development (18). Besides giving origin to SCs, they are known to differentiate into dental mesenchymal stem cells (19). Moreover, perivascular cells (20) and SCs (2) have been identified as two distinct sources of dental mesenchymal stem cells. SCs could mai-



tain mesenchymal stem cell reservoir in the dental pulp and participate in tooth development, self-renewal and injury repair (2). All support that SCs are closely linked to tooth development and injury repair.

The nervous and oral systems are evidently close in anatomical location, organogenesis and disease development. For tooth eruption (21), elongation of the root, dentin formation and response to stimulations from surroundings (22, 23), an intact nerve supply is required. In this study, we found that the PNS-related genes are closely related to tooth germ development based on the PPI analysis. Furthermore, the expression of SCs-associated genes showed the existence of different phenotypes of SCs, emphasizing the importance of SCs in tooth development. The whole process of SCs development involves SCPs, iSCs and mature SCs which are classified as mSCs and nmSCs. iSCs differentiate to pro-myelinating SCs that build a one-to-one relationship with large-caliber axons and finally transform into mature mSCs (24). In contrast, some nmSCs stay in contact with groups of small caliber axons and form so-called Remak bundles. Their morphology and antigenic marker expression, are similar to that of iSCs during development primarily (25). The development of SCs goes through different phenotypes that are adapted to support the balance between proliferation and differentiation (26).

From the beginning of tooth germ formation, iSCs/nmSCs exist in the ectoderm mesenchyme and gradually migrate into the enamel organ and DP, most obvious in the papilla. The results show that SCs may be involved in the neurodevelopment of tooth germs. SCs are mainly distributed in DP and SR in the late bell stage. Studies have shown that in the area where the ameloblasts are polarized in the enamel organ, capillaries are distributed in three regions: penetrate the outer epithelial layer of the enamel, cross and diverge with the SR layer and a large number of branches and anastomosis with SI (27). Due to the distribution of capillaries in SR and a large number of SCs existing in this period, it is speculated that SCs in SR may be the basis of the dental pulp nerve. During the entire tooth germ development process, SCs primarily exist in the phenotype of iSCs/nmSCs. This phenotype is a relatively stable and rapid proliferation phenotype (28), which may promote the further development of the tooth germ. Studies have found that although the proliferation rate of SCs precursors is very high, the maximum proliferation rate occurs in iSCs, which have similar performance in rats and mice (28, 29). We thus speculate that is the reason why most SCs exist as iSCs/nmSCs, mainly in the tooth development process. Furthermore, it has been reported that SCs were one of the sources of stem cells (2), which,

in conjunction with our findings, implies that iSCs/nmSCs may be the primary phenotype when combined with our findings.

Ca<sub>v</sub>1.2 is closely related to the tooth formation and osteogenesis. Our previous studies proved that knockdown of Ca<sub>v</sub>1.2 could inhibit the odontogenic differentiation of DPSCs (7) and the mineralization of rat DP stem cells (30). The results in the present study confirmed that SCs could differentiate into odontoblasts *in vitro*, and this differentiation process could be promoted after blocking LTCC with nimodipine. Contrary to our previous work (7), nimodipine inhibits the odontogenic differentiation of DPSCs. The possible reasons for this phenomenon can be explored from the two perspectives of cell characteristics and cellular life. DPSCs and SCs display different cell characteristics. Unlike non-excitabile DPSCs, SCs are excitable cells, in which the hydrolyzed distal C-terminus of Ca<sub>v</sub>1.2 could enter the nucleus to negatively regulate the gene transcription (31, 32). Ca<sub>v</sub>1.2 may function in a different way to regulate gene expression during the odontogenic differentiation of SCs. Secondly, Ca<sup>2+</sup> has been proven to be essential in each process of cellular life (i.e., survival, proliferation, differentiation, and death), while the high concentration of Ca<sup>2+</sup> is toxic to cells. In the process of odontogenic differentiation of SCs, there was a high probability of intracellular transient calcium accumulation, causing calcium overload and destroying intracellular calcium homeostasis. Several pieces of evidence indicate that calcium overload caused by intracellular calcium accumulation could inhibit the survival of SCs and remyelination (33, 34). Furthermore, nimodipine maintained at a concentration of 1~20 μM can exert a neuroprotective effect in the SCs culture (35-37), preventing the neuronal damage caused by the admission of Ca<sup>2+</sup> into the cells. These studies support the hypothesis that nimodipine may reduce the adverse effects of high calcium levels during odontogenic differentiation, thereby maintaining the survival and growth of SCs. In addition, the preservation of intracellular calcium homeostasis promotes better intercellular communication and interaction. Ca<sup>2+</sup> is essential for cell fates, which are regulated by a complex interplay between intracellular molecular regulatory networks and extracellular environmental stimuli as well. However, the quantity and intensity of nimodipine stimulation employed in our investigation may not be sufficient to cause a calcium-induced cell fate transition within SCs. Nimodipine may contribute more to maintaining calcium homeostasis, which is necessary for cell survival and growth and for the adequate differentiation of cultured SCs into odontoblasts during continuous odontogenic induction.

Not contradicting, in the later stage of odontogenic differentiation, the formation of mineralized nodules in the nimodipine-treated group was reduced. It is reasonable that the mineralization of the extracellular matrix (ECM) of dentin requires the odontoblasts to efficiently transfer calcium into the ECM (38). However, the continuous treatment of nimodipine blocked the LTCC pathway, interfering with calcium transport and reducing calcium nodule formation, as observed in our study and previous studies (7). Taken together, calcium may play different roles in different cells and various stages of cell differentiation. The specific role of calcium in the odontogenic differentiation of different cells is worth further study.

We used the PLP1-CreERT2/Rosa26-GFP tracing mice as the injury model and found that SCs participated in the dentine regeneration after damage, consistent with the results of Kaukua et al. (2). GFP<sup>+</sup> cells were almost absent in the control group, but GFP<sup>+</sup> cells gradually increased after injury. At 72 hours after injury, their expression was most apparent. They tended to the odontoblast layer near the injured site, showing that SCs of mice incisors' apex migrated from the deep pulp tissue to the odontoblast layer at the cusp injured site, which demonstrated that SCs proliferated, migrated, and differentiated into odontoblasts, and participated in the formation of the regenerative dentine.

Previous studies have confirmed that Ca<sub>v</sub>1.2 presents temporal and spatial expression characteristics in dental pulp after injury, and it also plays an important role in the repair process of dental pulp injury (8, 9). To further study the role of Ca<sub>v</sub>1.2 in the repair process of SCs after the dental pulp injury *in vivo*, we performed the immunofluorescence staining of Ca<sub>v</sub>1.2 in this model. The expression of Ca<sub>v</sub>1.2 presented a dynamic process after injury, consistent with the previous study, which reported the high expression of Ca<sub>v</sub>1.2 in the teeth injury lesion (9). In the control group, the expression of Ca<sub>v</sub>1.2 staining in the apical area was more robust than that in the cusp and the middle of the incisor. It was scattered in the pulp and was more prominent in the odontoblast layer. After injury, the expression of Ca<sub>v</sub>1.2 was enhanced in the cusp, middle and apical of the incisor. At 72 hours after injury, the expression was strongest and evenly in the pulp and weak in the odontoblast layer. At 5 days and 1 week after injury, the expression of Ca<sub>v</sub>1.2 in the odontoblast layer was significantly enhanced with the continuous growth of mice incisors. We speculated that it might be related to the active participation of odontoblasts in transporting and depositing calcium ions into mineralized areas during dentin formation. Importantly, we found that Ca<sub>v</sub>1.2 and SCs showed the same trend in the expression after injury

and co-expression in the neurovascular. Consistent with findings from Westenbroek et al. (9), who detected a considerable indication of Ca<sub>v</sub>1.2 in SCs after the molar damage, it suggests that Ca<sub>v</sub>1.2 might be implicated in the process of SCs participating in dentin regeneration after injury. The Ca<sub>v</sub>1.2 in SCs may therefore promote Ca<sup>2+</sup> influx into odontoblast-like cells, toward the front site of mineral production, in a similar manner to that of odontoblasts (39). Furthermore, Ca<sub>v</sub>1.2 expression in SCs may act as a second messenger for its interactions with surrounding cells or promote their proliferation and differentiation. Nevertheless, further research is necessary to determine if Ca<sub>v</sub>1.2 regulates calcium ions into SCs or SCs-derived odontoblast-like cells, which in turn affects dentine regeneration in response to tooth injury. Additionally, more research is still needed to fully understand the significance and function of Ca<sub>v</sub>1.2 in SCs.

In summary, SCs, as a part of PNS, play an essential role in tooth germ development. SCs have different phenotypes in different stages of tooth germ development. These phenotypes are coordinated in the whole process to ensure tooth development. Furthermore, SCs could be differentiated into odontoblasts *in vitro* and participate in the process of injured dental pulp repair as the source of mesenchymal cells, which is regulated by Ca<sub>v</sub>1.2. Our results provide important information on genes and molecules involved in tooth development, which could be further researched in the future.

#### ORCID

Jing He, <https://orcid.org/0009-0001-5085-4915>

Ting Wang, <https://orcid.org/0009-0008-2183-4457>

Danyang Liu, <https://orcid.org/0009-0008-8092-8170>

Jun Yang, <https://orcid.org/0000-0001-5445-0750>

Yuanpei He, <https://orcid.org/0000-0002-4168-4731>

Shouliang Zhao, <https://orcid.org/0000-0001-5960-9951>

Yanqin Ju, <https://orcid.org/0009-0001-0640-4124>

#### Funding

This research was supported by the National Natural Science Foundation of China (grant numbers 82071109, 82301056).

#### Potential Conflict of Interest

There is no potential conflict of interest to declare.

#### Authors' Contribution

Conceptualization: JH, TW, YJ, SZ. Data curation: JH, TW, DL, JY, YH. Formal analysis: JH, TW. Funding acquisition: YJ, SZ. Methodology: JH, TW. Project admin-

istration: YJ, SZ. Resources: YJ, SZ. Software: JH, TW, YJ. Supervision: YJ, SZ. Validation: YJ, SZ. Visualization: YJ, SZ. Writing – original draft: JH, TW. Writing – review and editing: JH, YJ, SZ.

## Supplementary Materials

Supplementary data including one supplementary data, three tables, seven figures, and supplementary methods can be found with this article online at <https://doi.org/10.15283/ijsc23205>

## References

- Miletich I, Sharpe PT. Normal and abnormal dental development. *Hum Mol Genet* 2003;12:R69-R73
- Kaukua N, Shahidi MK, Konstantinidou C, et al. Glial origin of mesenchymal stem cells in a tooth model system. *Nature* 2014;513:551-554
- Cristobal CD, Lee HK. Development of myelinating glia: an overview. *Glia* 2022;70:2237-2259
- D'Ascenzo M, Piacentini R, Casalbore P, et al. Role of L-type Ca<sup>2+</sup> channels in neural stem/progenitor cell differentiation. *Eur J Neurosci* 2006;23:935-944
- Wen L, Wang Y, Wang H, et al. L-type calcium channels play a crucial role in the proliferation and osteogenic differentiation of bone marrow mesenchymal stem cells. *Biochem Biophys Res Commun* 2012;424:439-445
- Linask KL, Linask KK. Calcium channel blockade in embryonic cardiac progenitor cells disrupts normal cardiac cell differentiation. *Stem Cells Dev* 2010;19:1959-1965
- Ju Y, Ge J, Ren X, et al. Ca<sub>v</sub>1.2 of L-type calcium channel is a key factor for the differentiation of dental pulp stem cells. *J Endod* 2015;41:1048-1055
- Fu Y, Ju Y, Zhao S. Ca<sub>v</sub>1.2 regulated odontogenic differentiation of NG2<sup>+</sup> pericytes during pulp injury. *Odontology* 2023;111:57-67
- Westenbroek RE, Anderson NL, Byers MR. Altered localization of Ca<sub>v</sub>1.2 (L-type) calcium channels in nerve fibers, Schwann cells, odontoblasts, and fibroblasts of tooth pulp after tooth injury. *J Neurosci Res* 2004;75:371-383
- Li J, Ju Y, Liu S, Fu Y, Zhao S. Exosomes derived from lipopolysaccharide-preconditioned human dental pulp stem cells regulate Schwann cell migration and differentiation. *Connect Tissue Res* 2021;62:277-286
- Direder M, Wielscher M, Weiss T, et al. The transcriptional profile of keloidal Schwann cells. *Exp Mol Med* 2022;54:1886-1900
- Chang SY, Chen RS, Chang JYF, Chen MH. The temporospatial relationship between mouse dental pulp stem cells and tooth innervation. *J Dent Sci* 2024;19:1075-1082
- Kanner AA, Marchi N, Fazio V, et al. Serum S100beta: a noninvasive marker of blood-brain barrier function and brain lesions. *Cancer* 2003;97:2806-2813
- Jessen KR, Brennan A, Morgan L, et al. The Schwann cell precursor and its fate: a study of cell death and differentiation during gliogenesis in rat embryonic nerves. *Neuron* 1994;12:509-527
- Yang Z, Wang KK. Glial fibrillary acidic protein: from intermediate filament assembly and gliosis to neurobiomarker. *Trends Neurosci* 2015;38:364-374
- García-Suárez O, Montaña JA, Esteban I, et al. Myelin basic protein-positive nerve fibres in human Meissner corpuscles. *J Anat* 2009;214:888-893
- Marty MC, Alliot F, Rutin J, Fritz R, Trisler D, Pessac B. The myelin basic protein gene is expressed in differentiated blood cell lineages and in hemopoietic progenitors. *Proc Natl Acad Sci U S A* 2002;99:8856-8861
- Le Douarin NM, Smith J. Development of the peripheral nervous system from the neural crest. *Annu Rev Cell Biol* 1988;4:375-404
- Nosrat IV, Widenfalk J, Olson L, Nosrat CA. Dental pulp cells produce neurotrophic factors, interact with trigeminal neurons *in vitro*, and rescue motoneurons after spinal cord injury. *Dev Biol* 2001;238:120-132
- Feng J, Mantesso A, De Bari C, Nishiyama A, Sharpe PT. Dual origin of mesenchymal stem cells contributing to organ growth and repair. *Proc Natl Acad Sci U S A* 2011;108:6503-6508
- Chidiac JJ, Kassab A, Rifai K, Saadé NE, Al Chaer ED. Modulation of incisor eruption in rats by sympathetic efferents. *Arch Oral Biol* 2018;89:31-36
- Li J, Parada C, Chai Y. Cellular and molecular mechanisms of tooth root development. *Development* 2017;144:374-384
- Duan Y, Liang Y, Yang F, Ma Y. Neural regulations in tooth development and tooth-periodontium complex homeostasis: a literature review. *Int J Mol Sci* 2022;23:14150
- Feltri ML, Poitelon Y, Previtali SC. How Schwann cells sort axons: new concepts. *Neuroscientist* 2016;22:252-265
- Jessen KR, Mirsky R. The origin and development of glial cells in peripheral nerves. *Nat Rev Neurosci* 2005;6:671-682
- Castelnuovo LF, Bonalume V, Melfi S, Ballabio M, Colleoni D, Magnaghi V. Schwann cell development, maturation and regeneration: a focus on classic and emerging intracellular signaling pathways. *Neural Regen Res* 2017;12:1013-1023
- Cerri PS, de Faria FP, Villa RG, Katchburian E. Light microscopy and computer three-dimensional reconstruction of the blood capillaries of the enamel organ of rat molar tooth germs. *J Anat* 2004;204:191-195
- Stewart HJ, Morgan L, Jessen KR, Mirsky R. Changes in DNA synthesis rate in the Schwann cell lineage *in vivo* are correlated with the precursor--Schwann cell transition and myelination. *Eur J Neurosci* 1993;5:1136-1144.
- Brown MJ, Asbury AK. Schwann cell proliferation in the postnatal mouse: timing and topography. *Exp Neurol* 1981;74:170-186
- Gao Q, Ge J, Ju Y, et al. Roles of L-type calcium channels (Ca<sub>v</sub>1.2) and the distal C-terminus (DCT) in differentiation and mineralization of rat dental apical papilla stem cells

- (rSCAPs). *Arch Oral Biol* 2017;74:75-81
31. Gao T, Cuadra AE, Ma H, et al. C-terminal fragments of the alpha 1C (Ca<sub>v</sub>1.2) subunit associate with and regulate L-type calcium channels containing C-terminal-truncated alpha 1C subunits. *J Biol Chem* 2001;276:21089-21097
  32. Gomez-Ospina N, Tsuruta F, Barreto-Chang O, Hu L, Dolmetsch R. The C terminus of the L-type voltage-gated calcium channel Ca(V)1.2 encodes a transcription factor. *Cell* 2006;127:591-606
  33. Yan JG, Agresti M, Zhang LL, Matloub HS, Sanger JR. Negative effect of high calcium levels on Schwann cell survival. *Neurophysiology* 2012;44:274-278
  34. Yan JG, Zhang LL, Agresti MA, et al. Effect of calcitonin on cultured Schwann cells. *Muscle Nerve* 2017;56:768-772
  35. Herzfeld E, Strauss C, Simmermacher S, et al. Investigation of the neuroprotective impact of nimodipine on Neuro2a cells by means of a surgery-like stress model. *Int J Mol Sci* 2014;15:18453-18465
  36. Herzfeld E, Speh L, Strauss C, Scheller C. Nimodipine but not nifedipine promotes expression of fatty acid 2-hydroxylase in a surgical stress model based on Neuro2a cells. *Int J Mol Sci* 2017;18:964
  37. Leisz S, Simmermacher S, Prell J, Strauss C, Scheller C. Nimodipine-dependent protection of Schwann cells, astrocytes and neuronal cells from osmotic, oxidative and heat stress is associated with the activation of AKT and CREB. *Int J Mol Sci* 2019;20:4578
  38. Chen Y, Koshy R, Guirado E, George A. STIM1 a calcium sensor promotes the assembly of an ECM that contains extracellular vesicles and factors that modulate mineralization. *Acta Biomater* 2021;120:224-239
  39. Lundgren T, Linde A. Voltage-gated calcium channels and nonvoltage-gated calcium uptake pathways in the rat incisor odontoblast plasma membrane. *Calcif Tissue Int* 1997; 60:79-85